

## PHYSICS AT CLIC\*

SOPHIE REDFORD, PHILIPP ROLOFF

on behalf of the CLICdp Collaboration

CERN, 1211 Geneva 23, Switzerland

*(Received May 4, 2015)*

CLIC is a concept for a future linear collider which would use two-beam acceleration to produce  $e^+e^-$  collisions with a centre-of-mass energy of 3 TeV. A staging scenario would also provide collisions at lower centre-of-mass energies, provisionally 350 GeV and 1.4 TeV. In order to demonstrate the wide range of physics processes available at such a linear collider, and to benchmark the performance of proposed detector models, a campaign of simulated physics analyses including Higgs, top and beyond the Standard Model processes has been undertaken at these three energy stages. These proceedings present the current status of these studies and illustrate the potential for precision physics measurements at CLIC.

DOI:10.5506/APhysPolB.46.1391

PACS numbers: 29.20.Ej, 14.80.Bn, 14.65.Ha, 11.30.Pb

**1. Introduction**

The Compact Linear Collider (CLIC) is an option for a future electron-positron collider, which would allow precision measurements of Standard Model (SM) Higgs and top processes in addition to providing sensitivity to beyond the SM (BSM) physics in a clean environment relative to hadron colliders [1, 2]. A two-beam acceleration technique would provide an accelerating gradient of 100 MV m<sup>-1</sup>, resulting in a total accelerator length of about 50 km for a centre-of-mass energy ( $\sqrt{s}$ ) of 3 TeV. A beam size of 40 nm  $\times$  1 nm in the transverse plane would provide an instantaneous luminosity of  $6 \times 10^{34}$  cm<sup>-2</sup> s<sup>-1</sup>. Dense trains of 312 bunches separated by 20 ms allow for power pulsing in the detector and a trigger-less readout. A polarised electron beam (80%) is planned, however unpolarised beams are assumed by default in the physics benchmark studies. Section 2 of these proceedings describes the CLIC Higgs capabilities, including single Higgs production,

---

\* Presented at the Cracow Epiphany Conference on the Future High Energy Colliders Kraków, Poland, January 8–10, 2015.

Higgs processes at higher energies, and a combined fit to all measured Higgs properties. Section 3 covers top physics, specifically the prospects for the top quark mass measurement at CLIC. Finally, Section 4 presents BSM physics at CLIC, illustrating both the possibility of direct searches for SUSY particles and indirect searches through precision measurements of known SM processes.

### 1.1. Energy stages

To provide optimised running conditions at different centre-of-mass energies, a staged construction is planned [3]. The energy stages are chosen to maximise the physics potential, and can be adapted to future discoveries at the LHC. The example scenario assumed here consists of three stages. The first energy stage, at  $\sqrt{s} = 350$  GeV, gives access to SM Higgs physics and provides the possibility of performing a  $t\bar{t}$  threshold scan. The second energy stage, at  $\sqrt{s} = 1.4$  TeV, provides sensitivity to many BSM models and gives higher statistics for measuring rarer Higgs processes including double Higgs production. The final energy stage, at  $\sqrt{s} = 3$  TeV, gives the best sensitivity to new physics and double-Higgs production, allowing improved measurements of the Higgs self-coupling and  $HHWW$  quartic coupling.

### 1.2. Beam-induced background

The small size of the beams in conjunction with high bunch populations ( $\mathcal{O}(10^9)$ ) and high beam energies gives rise to challenging levels of beam-induced backgrounds, produced when incoming bunches accelerate in each other's electromagnetic fields and radiate photons. These photons can interact with each other or the oncoming beam, producing hadrons and  $e^+e^-$  pairs. Produced background particles tend to continue forward inside the beam pipe. However, some do interact with the detector; at  $\sqrt{s} = 3$  TeV, there will be 3.2  $\gamma\gamma \rightarrow$  hadrons interactions for every bunch crossing, depositing  $\sim 20$  TeV of energy per bunch train into the calorimeters. Rejecting these background particles is possible using momentum and timing cuts, which drives challenging requirements on detector timing capabilities.

### 1.3. Detector models

Two detector models were used in the studies presented here, both based on ILC detector concepts [4, 5] and adapted for the higher centre-of-mass energies at CLIC. The principle difference between the two models concerns the tracking system; CLIC\_ILD proposes a TPC [6], whereas CLIC\_SiD plans for a full silicon tracker [7]. Otherwise, both detector designs comprise of a pixelated low mass vertex detector, finely segmented electronic and

hadronic calorimeters designed to perform particle flow analysis, a strong solenoidal field of 4–5 T, an instrumented return yoke and a complex forward region including final focusing magnets and additional calorimeters.

#### 1.4. Simulation and reconstruction framework

The studies presented in these proceedings were performed using full simulation and reconstruction of all physics processes and relevant backgrounds, including beam-induced backgrounds. The WHIZARD event generator [8, 9] is employed, followed by PYTHIA [10] for hadronisation and TAUOLA [11] for tau decays. GEANT4 [12, 13] is used to simulate the detector response. Particle flow reconstruction is performed [14, 15]. Jet clustering is performed using FASTJET [16], where the longitudinally invariant  $k_T$  algorithm with two additional beam jets was found to give good performance. LCFIPlus [17] is used for flavour-tagging.

## 2. Higgs physics at CLIC

Studying the properties of the newly-discovered Higgs boson [18, 19] in the relatively clean environment of electron–positron collisions would be a priority for CLIC. This section details studies of single Higgs production and decay modes, double Higgs production, the top Yukawa coupling and how all measurements can be combined in a model-independent fit.

### 2.1. Single Higgs production

An electron–positron collider with staged centre-of-mass energies up to 3 TeV would provide access to many Higgs production modes, as seen in Fig. 1 (left). At  $\sqrt{s} = 350$  GeV, the dominant Higgs production process is Higgsstrahlung, in which a Higgs is radiated off a  $Z$  boson. At the higher centre-of-mass energy stages,  $WW$ -fusion becomes the principle production mode, with the cross section for  $ZZ$ -fusion also rising with centre-of-mass energy about one order of magnitude lower.

Large samples of Higgs bosons would be collected at CLIC. With an integrated luminosity of  $500 \text{ fb}^{-1}$  at  $\sqrt{s} = 350$  GeV, around 70,000 Higgsstrahlung events would be produced. The expected  $1.5 \text{ ab}^{-1}$  and  $2 \text{ ab}^{-1}$ , each collected in  $\sim 4$  years at 1.4 TeV and 3 TeV respectively, together produce over a million  $WW$ -fusion events. The polar angle of the Higgs bosons produced in these two processes differs (see Fig. 1 (right)), with Higgsstrahlung producing Higgs bosons centrally in the detector and vector–boson fusion resulting in forward Higgs bosons at high energy. Therefore, measurements at the higher energy stages drive the development of high-resolution tracking and calorimetry down to low polar angles in the forward regions.

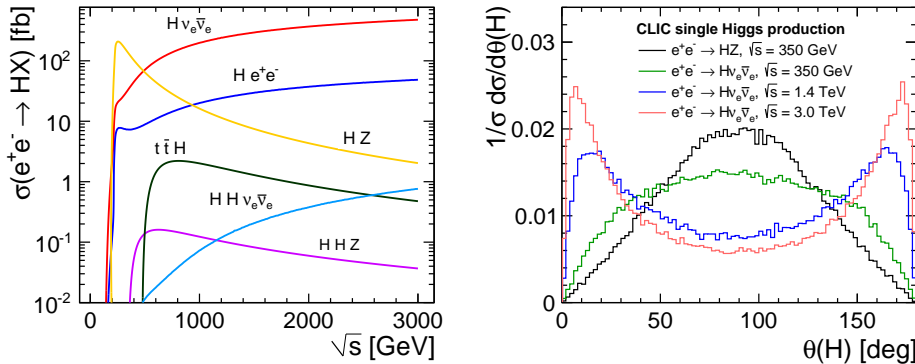


Fig. 1. Left: Cross section as a function of centre-of-mass energy for various Higgs production processes available at CLIC. Taken from [2]. Right: Polar angle of the Higgs produced in Higgsstrahlung and vector–boson fusion events.

The Higgsstrahlung production mode at  $\sqrt{s} = 350$  GeV gives the opportunity to perform a completely model-independent measurement of the  $HZZ$  coupling at CLIC. By using the  $Z$ -recoil mass only to identify  $HZ$  events, this technique makes no assumptions of the Higgs decay mode, and is sensitive to invisible decays. The uncertainty on the  $HZZ$  coupling is calculated to be 2%, using only  $e^+e^- \rightarrow ZH \rightarrow l^+l^-H$  events, where  $l = e, \mu$ . A substantial improvement can be gained from using the additional statistics in hadronic  $Z$  decays, although the reconstruction efficiency of the  $Z$  then depends slightly on the Higgs decay mode. However, it was found that even extreme variations of the SM Higgs branching fractions led to a systematic uncertainty less than half the size of the statistical uncertainty. Using hadronic  $Z$  decays, the uncertainty on the  $HZZ$  coupling was found to be 0.9%. Combined, the two channels give an uncertainty of 0.8% on the  $HZZ$  coupling. This analysis also enables the branching ratio of Higgs to invisible decays to be constrained to  $\text{BR}(H \rightarrow \text{invis.}) < 1\%$  at 90% confidence level.

## 2.2. Higgs production at higher energies

Single Higgs production at higher energies enables more precise measurements of cross section  $\times$  branching ratio. The simultaneous analysis of  $H \rightarrow b\bar{b}/c\bar{c}/g\bar{g}$  relies on the separation of the different hadronic final states by flavour-tagging. This is extremely challenging at hadron colliders, but at CLIC uncertainties on the charm and gluon channels of a couple of % are achievable. In addition, the Higgs mass can be extracted from the  $b\bar{b}$  decay channel with a precision of  $\pm 33$  MeV at  $\sqrt{s} = 3$  TeV (see Fig. 2 (left)).

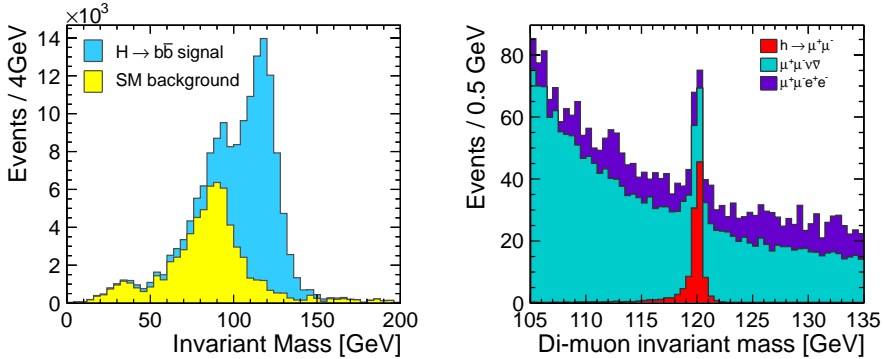


Fig. 2. Left: Reconstructed, selected  $b\bar{b}$  invariant mass peak in the  $H \rightarrow b\bar{b}$  decay channel. Right: Reconstructed, selected di-muon invariant mass peak in the  $H \rightarrow \mu^+\mu^-$  decay channel. Both taken from [2].

The increased Higgs production cross sections at higher energies also provide sufficient statistics to study rarer decay modes such as  $H \rightarrow \mu^+\mu^-$ ,  $H \rightarrow \gamma\gamma$  and  $H \rightarrow Z\gamma$ . All of these decay modes have branching ratios at the sub-‰ level. The di-muon final state requires excellent tracking resolution to ensure that the signal peak is as narrow and significant as possible (see Fig. 2 (right)). At  $\sqrt{s} = 3$  TeV, CLIC would achieve an uncertainty on  $\sigma(H\nu_e\bar{\nu}_e) \times \text{BR}(H \rightarrow \mu^+\mu^-)$  of 16%. Similar uncertainties are achieved for the other two channels; 15% for  $\gamma\gamma$  at  $\sqrt{s} = 1.4$  TeV and 42% for  $Z\gamma$  at  $\sqrt{s} = 1.4$  TeV. Sensitivity to these very rare decays demonstrates the excellent background rejection and reconstruction efficiency possible at CLIC.

At  $\sqrt{s} = 1.4$  TeV, the top Yukawa coupling can be measured directly using  $t\bar{t}H$  production, in which a top quark radiates a Higgs boson. In the SM, this coupling is the strongest Higgs-fermion coupling, as the top quark is the most massive fermion. The Higgs decay to  $b\bar{b}$  is analysed, resulting in an eight fermion final state including four  $b$ -jets. This analysis is therefore an excellent detector benchmark test, requiring accurate jet clustering, lepton identification and flavour-tagging. Using the fully-hadronic and semi-leptonic final states, the statistical uncertainty on the cross section was measured to be 8.4%. Taking into account the identical final state produced by Higgsstrahlung followed by  $t\bar{t}$  production, this translates to an uncertainty on the top Yukawa coupling of 4.5%.

At high centre-of-mass energies, the  $HH\nu_e\bar{\nu}_e$  cross section gives sensitivity to the Higgs self-coupling and the quartic  $HHWW$  coupling. High energy and high luminosity are of crucial importance for these analyses, as only 225 (1200)  $e^+e^- \rightarrow HH\nu_e\bar{\nu}_e$  events are expected in  $1.5 \text{ ab}^{-1}$  ( $2 \text{ ab}^{-1}$ )

at  $\sqrt{s} = 1.4$  TeV (3 TeV). Optimising only for the  $b\bar{b}b\bar{b}$  final state, the Higgs self-coupling would be measured at  $\sqrt{s} = 1.4$  TeV with a precision of 32%. At  $\sqrt{s} = 3$  TeV, CLIC can achieve 16% precision, which is reduced to 12% if a polarised electron beam (at  $-80\%$ ) is used. The quartic coupling could be measured with 3% (7%) precision at  $\sqrt{s} = 3$  TeV (1.4 TeV) using unpolarised beams. These analyses may be repeated, so as to also optimise for the  $b\bar{b}WW$  final state.

### 2.3. Combined Higgs fit

The Higgs couplings and decay width can be determined in a combined fit to all of the measurements performed at the three energy stages of CLIC. This fully model-independent method is only possible at a lepton collider, and stems from the model-independent measurement of the  $HZ$  cross section. Figure 3 (left) illustrates the precision on the Higgs couplings and decay width achieved by the full CLIC programme, showing that couplings can be determined at the %-level. The Higgs width is extracted with 3.5% precision.

Performing this combination in the same manner as the LHC experiments (requiring no unknown decays) improves the precision dramatically, for example, the uncertainty on the decay width is sub-% level after the full CLIC programme (see Fig. 3 (right)). However, the results of this fit are strongly dependent on the starting assumptions.

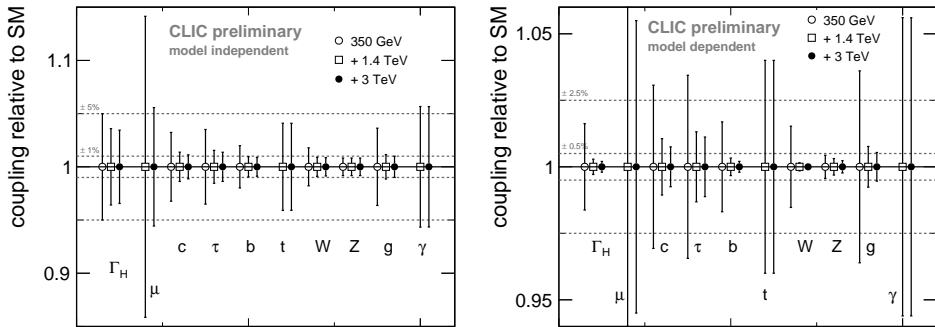


Fig. 3. Illustration of the achievable precision on the Higgs couplings and decay width after three successive CLIC energy stages. Left: For a model-independent combined fit. Right: For a model-dependent combined fit. Results at  $\sqrt{s} = 1.4$  TeV and 3 TeV are scaled to reflect  $-80\%$  electron beam polarisation.

2.4. Future analyses: CP properties of the Higgs

CLIC also has a potential to measure CP properties of the Higgs. One opportunity would be to use  $t\bar{t}H$  events, extending the existing  $t\bar{t}H$  study to include a measurement of the polarisation asymmetry of the top quark and the up–down asymmetry [20]. Another possibility would be to use vector–boson fusion events, using angular variables to determine whether the Higgs is an admixture of CP odd and even states [21].

3. Top physics at CLIC

In addition to a broad and comprehensive Higgs physics programme, CLIC would also give the opportunity to study the top quark with unprecedented precision, not least because CLIC offers the exciting prospect of producing  $t\bar{t}$  pairs for the first time in  $e^+e^-$  collisions.

3.1. Top quark mass measurement

Dedicated operation during the first energy stage would enable a  $t\bar{t}$  threshold scan to be performed at CLIC, resulting in a measurement with a theoretically clean interpretation of the top quark mass [22]. Collecting  $10 \times 10 \text{ fb}^{-1}$  of data in steps around  $\sqrt{s} = 350 \text{ GeV}$  would allow the  $t\bar{t}$  production cross section to be measured as a function of centre-of-mass energy (Fig. 4 (left)). The statistical uncertainty on the measured top mass using this method is 34 MeV. The total uncertainty, including the theoretical uncertainty and systematic uncertainties on the beam energy, luminosity spectrum and background subtraction, is below 100 MeV. The strong coupling constant  $\alpha_s$  could also be extracted with high precision, see Fig. 4 (right).

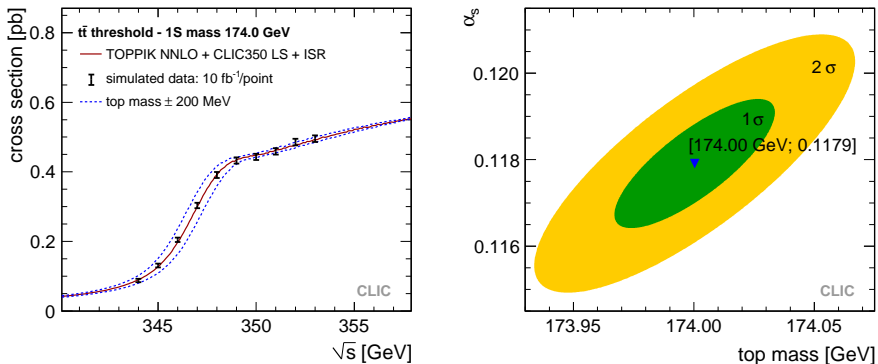


Fig. 4. Left: Cross section as a function of centre-of-mass energy for  $t\bar{t}$  production. Right: Correlation between the top mass and  $\alpha_s$ , the strong coupling constant. Both taken from [22].

## 4. Physics beyond the Standard Model at CLIC

Strategies for studying BSM physics at CLIC follow two different approaches, depending on the nature of the new physics involved [21]. Direct pair production of new particles is possible up to the kinematic limit of  $\sqrt{s}/2$ . In this area, CLIC is especially sensitive to electroweak states, and so complementary to the LHC. Much higher mass scales are attainable through indirect searches, where precision measurements of observables are compared to SM expectations.

### 4.1. Direct searches for BSM physics

The studies of direct searches make use of three SUSY models [2, 3], which contain sparticles with masses within the kinematic limit of CLIC. A simple example of a direct search involves reconstructing sleptons at  $\sqrt{s} = 3$  TeV. Channels such as  $e^+e^- \rightarrow \tilde{\mu}_R^+ \tilde{\mu}_R^- \rightarrow \mu^+ \mu^- \tilde{\chi}_1^0 \tilde{\chi}_1^0$  result in high energy leptons and missing energy. The masses of the sleptons can be determined by taking the endpoints of the energy spectra of such processes, as seen in Fig. 5 (left). This results in uncertainties of a few GeV, for slepton masses in the range of 1 TeV.

A similar strategy can be employed for gauginos produced at  $\sqrt{s} = 3$  TeV. Chargino and neutralino pair production, for example  $e^+e^- \rightarrow \tilde{\chi}_1^+ \tilde{\chi}_1^- \rightarrow \tilde{\chi}_1^0 \tilde{\chi}_1^0 W^+ W^-$ , results in signals of pairs of bosons and missing energy. Reconstructing the four jets (see Fig. 5 (right)) and pairing them to form  $W$ ,  $Z$  and  $H$  results in precisions on the measured gaugino masses of 1%, for sparticle masses of a few hundred GeV.

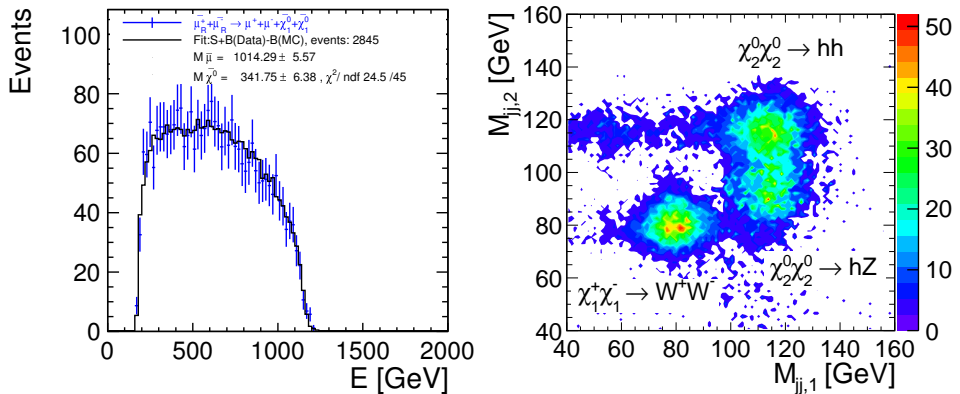


Fig. 5. Left: Reconstructed energy spectrum from slepton decays. Right: Reconstructed di-jet masses from gaugino decays. Both taken from [2].

An example of complex final states in direct BSM searches concerns heavy Higgs bosons, which decay to  $b\bar{b}$  or  $t\bar{t}$  depending on their charge. Separating heavy Higgs bosons which are almost degenerate in mass requires determining the jet substructure in order to tag heavy flavour jets. This is possible at CLIC due to the finely segmented calorimeters, and results in heavy Higgs mass measurements accurate to sub-% level (see Fig. 6).

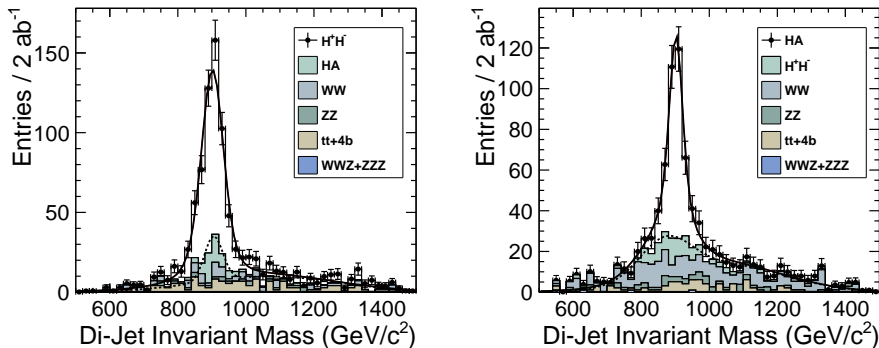


Fig. 6. Heavy Higgs bosons produced at  $\sqrt{s} = 3$  TeV, which are almost degenerate in mass. Left: The charged  $H^+H^-$ , decaying to  $t\bar{t}$  pairs. Right: The neutral  $HA$ , decaying to  $b\bar{b}$  pairs. Both taken from [2].

Although these direct searches use SUSY particles as an example, the analyses have a wider applicability to new physics. Since the new particles are states which can be fully classified by their mass, spin and quantum numbers, sensitivity to them will hold no matter what model of new physics describes them.

#### 4.2. Sensitivity of precision measurements to BSM physics

New physics beyond the kinematic limit of CLIC could still be detected due to its effect on known SM observables. One opportunity concerns the process  $e^+e^- \rightarrow \mu^+\mu^-$ , which is sensitive to the presence of a high mass  $Z'$  boson. Observables such as the total cross section, the forward-backward asymmetry and the left-right asymmetry (with  $\pm 80\%$  electron polarisation) give a discovery reach up to tens of TeV at CLIC (see Fig. 7 (left)) [23].

Another possibility concerns composite Higgs models, in which the Higgs boson exists as a composite state of bound fermions. Using only the results from single Higgs production, CLIC could significantly reduce the composite space and would provide an indirect probe up to a Higgs composite scale of 70 TeV (see Fig. 7 (right)) [24].

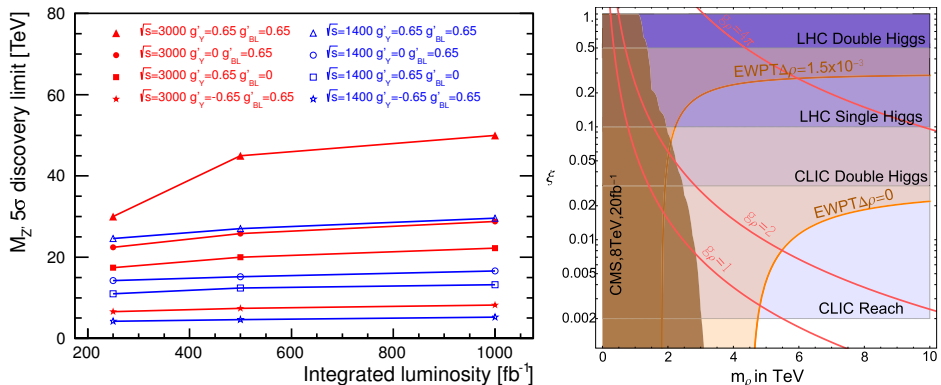


Fig. 7. Left:  $Z'$  mass  $5\sigma$  discovery limit as a function of integrated luminosity, for different BSM models. Taken from [21]. Right: Constraints and prospects for ruling out a composite Higgs boson. For more details, see [21]. Taken from [24].

#### 4.3. Future analyses: physics beyond the Standard Model

Many SUSY signatures of interest have yet to be studied at CLIC, including Higgsinos with small mass splittings. This analysis is of particular interest as a detector benchmark test, since the signal includes soft particles which would be challenging to identify in the presence of beam-induced backgrounds. Another SUSY decay of interest is stop to top decays, which produces boosted top quarks.

Additional BSM searches could be performed at CLIC, for instance a model-independent search for Dark Matter using the  $\gamma +$  missing energy final state, generalised searches for higher-dimensional effective operators, hidden sectors, or weakly interacting exotica. A crucial point is that CLIC is ready to respond to the theoretical interpretation of any BSM physics indications in Run 2 LHC data.

Finally, precision measurements of SM processes could be employed at CLIC as tools for studying BSM. With their extremely high mass, top quarks make excellent probes for new physics through observables such as the forward–backward asymmetry and CKM matrix element  $V_{tb}$ . Similarly, precision electroweak measurements can act as a window onto new physics, for example triple and quartic gauge couplings and the  $W$  mass measurement. Large samples of single  $W$  events will be produced at high energy CLIC, giving the opportunity to make a competitive  $W$  mass measurement using the hadronic final state.

## 5. Summary

To summarise, CLIC offers a strong SM physics programme throughout its three energy stages. At the first energy stage of  $\sqrt{s} = 350$  GeV, precise measurements of many Higgs couplings and branching ratios can already be made. Higher energy stages (up to  $\sqrt{s} = 3$  TeV) give access to rarer Higgs decay modes, in addition to  $t\bar{t}H$  and double-Higgs production. All Higgs measurements are combined in a model-independent simultaneous fit, with sub-% level precision on many measurements. Top physics is also accessible, in particular by using a threshold scan to achieve unprecedented precision on the top quark mass.

High energy CLIC provides significant potential for studying BSM phenomena, either by providing further measurements of LHC discoveries or by acting as a discovery machine in its own right. Direct production of new particles is possible up to the kinematic limit of 1.5 TeV, with subsequent decays to SM particles allowing use of, for example, the end-point mass measurement technique. Indirect measurements, such as the asymmetry of  $e^+e^- \rightarrow \mu^+\mu^-$ , increase the mass reach of CLIC up to tens of TeV.

## REFERENCES

- [1] M. Aicheler *et al.*, Technical Report CERN-2012-007, SLAC-R-985, KEK-Report-2012-1, PSI-12-01, JAI-2012-001.
- [2] A. Miyamoto, M. Stanitzki, H. Weerts, L. Linssen, Technical Report, [arXiv:1202.5940](#) [[physics.ins-det](#)].
- [3] P. Lebrun *et al.*, Technical Report, [arXiv:1209.2543](#) [[physics.ins-det](#)].
- [4] T. Abe *et al.*, Technical Report, [arXiv:1006.3396](#) [[hep-ex](#)].
- [5] H. Aihara, P. Burrows, M. Oreglia, Technical Report, [arXiv:0911.0006](#) [[physics.ins-det](#)].
- [6] A. Muennich, A. Sailer, Technical Report LCD-Note-2011-002.
- [7] C. Greife, A. Muennich, Technical Report LCD-2011-009.
- [8] W. Kilian, T. Ohl, J. Reuter, *Eur. Phys. J. C* **71**, 1742 (2011).
- [9] M. Moretti, T. Ohl, J. Reuter, Technical Report, [arXiv:hep-ph/0102195](#).
- [10] T. Sjostrand, S. Mrenna, P.Z. Skands, *J. High Energy Phys.* **0605**, 026 (2006).
- [11] Z. Was, *Nucl. Phys. Proc. Suppl.* **98**, 96 (2001).
- [12] S. Agostinelli *et al.*, *Nucl. Instrum. Methods Phys. Res. A* **506**, 250 (2002).
- [13] J. Allison *et al.*, *IEEE Trans. Nucl. Sci.* **53**, 270 (2006).
- [14] M.A. Thomson, *Nucl. Instrum. Methods Phys. Res. A* **611**, 25 (2009).
- [15] J.S. Marshall, A. Munnich, M.A. Thomson, *Nucl. Instrum. Methods Phys. Res. A* **700**, 153 (2012).

- [16] M. Cacciari, G. Salam, G. Soyez, *Eur. Phys. J. C* **72**, 1896 (2012).
- [17] LCFIPlus,  
<https://confluence.slac.stanford.edu/display/ilc/LCFIPlus>
- [18] G. Aad *et al.*, *Phys. Lett. B* **716**, 1 (2012).
- [19] S. Chatrchyan *et al.*, *Phys. Lett. B* **716**, 30 (2012).
- [20] R. Godbole *et al.*, *Eur. Phys. J. C* **71**, 1681 (2011).
- [21] H. Abramowicz *et al.*, Technical Report, [arXiv:1307.5288](https://arxiv.org/abs/1307.5288) [hep-ex].
- [22] K. Seidel, F. Simon, M. Tesar, S. Poss, *Eur. Phys. J. C* **73**, 2530 (2013).
- [23] J.-J. Blaising, J.D. Wells, Technical Report, [arXiv:1208.1148](https://arxiv.org/abs/1208.1148) [hep-ph].
- [24] R. Contino *et al.*, *J. High Energy Phys.* **1402**, 006 (2014).